

Research Article

Electroacupuncture Improves Antidepressant Effects in CUMS Rats by Protecting Hippocampal Synapse and Mitochondrion: An Ultrastructural and iTRAQ Proteomic Study

Jialing Zhang,¹ Zhinan Zhang ,² Jiping Zhang,² Zheng Zhong,³ Zengyu Yao,² Shanshan Qu ,² and Yong Huang ²

¹School of Chinese Medicine, The University of Hong Kong, 999077, Hong Kong

²School of Traditional Chinese Medicine, Southern Medical University, Guangzhou, Guangdong Province 510515, China

³Nanfang Hospital, Southern Medical University, Guangzhou, Guangdong Province 510515, China

Correspondence should be addressed to Shanshan Qu; s2qu@163.com and Yong Huang; nanfanglihuang@163.com

Received 27 November 2018; Accepted 4 April 2019; Published 17 April 2019

Academic Editor: Gerhard Litscher

Copyright © 2019 Jialing Zhang et al. This is an open access article distributed under the Creative Commons Attribution License, which permits unrestricted use, distribution, and reproduction in any medium, provided the original work is properly cited.

Electroacupuncture (EA) is considered a complementary therapy for depression. Trials also found that EA has additive benefits when combined with medication compared with medication alone. It is revealed that EA restores altered hippocampal synaptic plasticity in depressed brain. But precise molecular mechanism is poorly understood. Here, we evaluated the therapeutic effects of EA and EA combined with selective serotonin reuptake inhibitor (SSRI) on depressed (CUMS) rats. Then a new proteomics approach, isobaric tag for relative and absolute quantitation (iTRAQ), was used to explore the differential expressed synaptic protein in hippocampus between CUMS and EA-treated rats to identify the possible target molecular mechanism of its effects. We found that EA had additive benefit against depressive behaviors when combined with SSRI. Ultrastructure study on neuron showed significant change in postsynapse density (PSD) and mitochondrion. Through iTRAQ, it is found that synaptic and mitochondrial proteins were significantly changed after EA, consisting with ultrastructure study results. These findings suggest that EA improves antidepressant performance in depressed rats through protecting synaptic and mitochondrial functions in hippocampus.

1. Introduction

Although antidepressants instantly increase levels of monoamines between synapse clefts, it takes weeks until symptoms alleviation [1, 2]. Besides, the efficacy of antidepressants may be outweighed by their adverse health effects [3]. Therefore, therapies that overcome these limits are rather expected.

Electroacupuncture (EA) is a form of acupuncture where a small electric current is passed between pairs of acupuncture needles [4, 5]. Findings suggest that EA combined with antidepressant brings the symptomatic improvement of antidepressants treatment forward within 1-2 weeks with less adverse health effects of antidepressant [6, 7]. Moreover, our previous RCT study shows that combining EA (at GV20 and GV29) with paroxetine (a widely used SSRI) improves depressive symptoms within at least 1 week and the therapeutic effects continue even after the therapy [8, 9].

Therefore, combination therapy of EA and antidepressants is a promising strategy against depression.

Hippocampal volume loss is one of the neuroanatomical characters of depression [10, 11]. Thus, hippocampus is considered as a diagnostic neurobiomarker and a therapeutic target for depression [12]. MRI researches also prove that hippocampus is one of the target brain regions of EA in depressed patients [13–15].

A prominent feature of hippocampus is synaptic plasticity [16, 17]. Recent studies have called attention to the role of altered hippocampal synaptic plasticity in the biology of depression. It is showed that chronic stress reduces synaptic and dendritic plasticity. Moreover, depressed subjects show evidence of impaired neuroplasticity and antidepressant medications enhance neuroplasticity at both a molecular and a dendritic level. These findings suggest that disrupted synaptic plasticity is an underlying feature of depression

[18, 19]. Besides, mitochondria are enriched at synapse as supporting organelles. It is also revealed that mitochondria play an active role in synaptic plasticity through multiple pathways [20]. Researches show that EA relieves depression by restoring hippocampus synaptic plasticity in hippocampus through increasing glutamate receptor or decreased serotonin receptor, proposing the importance of hippocampal synaptic plasticity in the acting mechanism of EA [21–23]. Researches also show that EA intervention can reverse mitochondria damage in depressed hippocampus [24]. However, there exact molecular mechanism remains largely to be discussed. We therefore sought to thoroughly investigate synaptic as well as mitochondrial proteins involved in the synaptic regulation of EA on depressed hippocampus.

Proteomic technologies are the ideal techniques for the detection and investigation of biomarker candidates, owing to the high sensitivity and analytical performance that can be achieved and the ability to generate large datasets through identification of large and ever-increasing numbers of proteins [25–27]. Isobaric tag for relative and absolute quantitation (iTRAQ) is a proteomics approach which can determine the amount of proteins from different sources in a single experiment [28]. This technology has been used to outline the proteomics profiles of cancers [29]. Currently, a number of biomarkers have been detected in urine and tissue for bladder cancer using this technique [30]. Therefore, we used iTRAQ to thoroughly explore the mechanism of EA's effects on hippocampal synaptic plasticity in depression.

In this study, we perform EA at GV20 (Baihui) and GV29 (Yintang) in depressed (CUMS) rats, using behavioral tests to monitor the effects of EA on depressive-like symptoms. We also observed the synaptic ultrastructure differences between CUMS and EA hippocampal neurons. iTRAQ was used to identify the differentially expressed hippocampal synaptic proteins between CUMS and EA rats to identify candidate proteins responsible for the therapeutic effects of EA on depression.

2. Material and Methods

2.1. Animals. 70 male Wistar rats (weight 200 ± 20 g, 6–7-week-old, Experimental Animal Center of Southern Medical University) were housed in individual cages under a 12–12 h light/dark cycle in a standard SPF facility (temperature $24 \pm 2^\circ\text{C}$; humidity 50%–60%) with access to food and water ad libitum. Before we started the experiment, rats were allowed to habituate for 6 days. Rats were randomly assigned into 5 groups: control, CUMS, SSRI, EA, and EA+SSRI groups ($n=10-15$ rats/group). All the experimental procedures were performed in accordance with the National Institutes of Health Guide for the Care and Use of Laboratory Animals and the procedures were approved by the Ethics Committee on Animal Experimentation of Southern Medical University. All efforts were made to minimize animal suffering and to reduce the number of animals used.

2.2. CUMS Paradigm. To develop a CUMS rat model, rats were exposed to 10 different kinds of stressors over a period of

21 days, 1 stressor per day (Figure 1(a)). All of these stressors were random arranged, which include water deprivation (24 h), food deprivation (24 h), wet bedding (24 h), light-dark reversal (24 h), Stroboscopic lighting (12h), immobilization (2 h), cold swim (4°C , 5min), warm swim (45°C , 5min), level shaking (5min), and tail clamping (3min) [31, 32].

2.3. Interventions. After CUMS paradigm, rats in EA group underwent EA at GV20 (above the apex auriculate, on the midline of the head) and GV29 (at the middle point between the eyes) (Figure 1(b)) [33]. Rats were lightly immobilized with plastic fixator. Then disposable acupuncture needles ($0.30\text{mm} \times 25\text{mm}$, Hua Tuo Appliance Factory) were inserted in both acupoints obliquely to 5mm depth. Following the insertions, electrodes were added to the handle of the needles using 1mA, 2Hz, and 5Hz, electrical stimulation for 30 mins each time, once per day for 7 consecutive days. EA rats were also given saline (same volume per kg as paroxetine). Rats in SSRI group were given paroxetine (1.8mg/kg/d) [34, 35] after 30-minute immobilization for 7 consecutive days. Rats in EA+SSRI group were given both EA intervention and paroxetine once per day for 7 consecutive days. For the CUMS group and control group, we only performed lightly immobilization and saline administration, once per day during the same period.

2.4. Behavioral Assessments. In sucrose preference test (SPT), rats were subjected to a 2-day habituation phase before the actual test phase. In the 3rd day, food and water were removed for a deprivation period of 23 h. The following morning, test phase began, during which customized drinking bottles filled with either 1 % sucrose solution or water were given to the rats for 1 h. Sucrose preference rate was calculated as the amount of sucrose solution relative to the total fluid consumption [36].

In open field test (OFT), we used an arena with walls in a quiet and dimly lighted room as the open field (OF). The field was divided into 25 equally with grids and square crossings. Center zone dominated the 9 grids in center, and other 16 grids belonged to peripheral zone. Each rat was put in the center of the OF for a period a 5mins, during which the tester left the room. We used video cameras with associated software (Smart 2.0) to automate the assessment process. Behavioral patterns measured include time in central zone and total travel distance [37].

Behavioral tests and weight assessment were performed after intervention termination.

2.5. Tissue Processing. After animals were anesthetized with 25% pentobarbital sodium (50mg/kg, intraperitoneal injection), we used cervical dislocation to prevent pre- and post-synaptic effects of anesthesia. Animals were decapitated and the brains were instantly dissected with all attached tissues removed. Hippocampus tissues were removed and rinsed with pre-cold phosphate-buffered saline (PBS). Removed tissues of 3 rats/group were immediately snap-frozen within liquid nitrogen and stored in refrigerator (-80°C) until isobaric labeling. 6 rats/group were transferred into in the

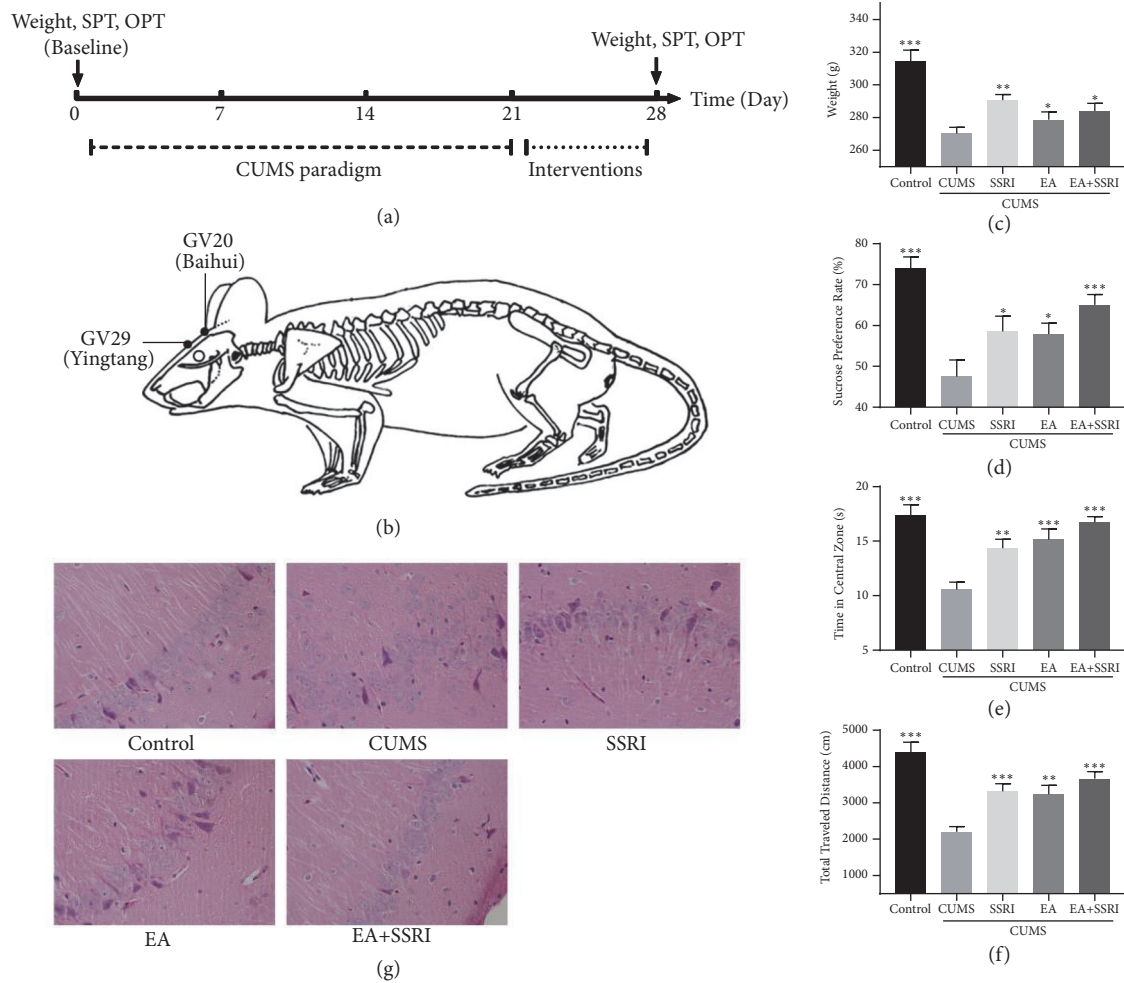


FIGURE 1: EA+SSRI accelerates depressed-like behaviors improvement in depressed rats. (a) Timeline of CUMS paradigm, interventions, and behavioral tests. (b) EA was performed at acupuncture point GV20 (Baihui) and GV29 (Yingtang). (c) EA and EA+SSRI increased body weight change caused by CUMS. (d) Both EA and EA+SSRI increased sucrose preference rate in depressed rats. EA+SSRI increased sucrose preference significantly. (e) EA and EA+SSRI increased central zone time spent in depressed rats significantly. (f) CUMS-induced total traveled distance decrease in open field was reversed by EA and EA+SSRI. EA+SSRI increased total traveled distance significantly (n=10-15 rats/group). (g) EA+SSRI reverses the hippocampal histopathology changes during CUMS (n=6 rats/group), $\times 400$. Bar graphs represent mean \pm SE. *: $P < 0.05$, **: $P < 0.01$, and ***: $P < 0.001$ vs. CUMS. One-way ANOVA with LSD post hoc test.

fixative (4% paraformaldehyde; 0.1 M phosphate buffer at pH 7.4) until electron microscopy and HE stain.

2.6. Electron Microscopy. Tissues were microwaved at full power (700W microwave oven) for 10 s to enhance penetration of the fixative through the depth of the slice with a final temperature of $< 35^{\circ}\text{C}$. Slices were left overnight in the same fixative and then rinsed with 0.1M phosphate buffer (4 \times for 15 min). First, they were immersed in 1% osmium for 1 hour and rinsed in buffer (3 \times for 15 min). Next, they were immersed in ascending concentrations of acetone (50, 70, 90, and 100%). Finally, they were quickly immersed in Spurr's resin at room temperature overnight and then embedded in coffin molds in Spurr's resin and cured for 8 hours at 70°C in an oven. They were then vibrasliced at 60 nm (Leica UC7, Leica). Ultrathin sections were counterstained with saturated aqueous uranyl acetate, followed by Reynolds lead citrate for 5 min. Sections

were photographed with a transmission electron radiography (Hitachi H-7500, Hitachi) at 5,000 \times magnification.

2.7. Sample Preparation and Isobaric Labeling. Equal amounts of each hippocampus sample were pooled to produce a sample group. Samples were randomly mixed into a sample group as a biological replicate. The hippocampus samples were reduced and then alkylated, followed by determination of protein concentration in the samples using bicinchoninic acid assay (H4MFPTAD, BioTek). 100 mg protein from each sample was digested with trypsin (Promega) overnight at 37°C . The pH was monitored to assure a complete digestion. After trypsin digestion, different sample peptides resolved in 0.5 M TEAB (Sigma) were labeled with different isobaric tags according to the protocol of the iTRAQ Reagent-8plex Multiplex Kit (AB SCIEX). Briefly, one unit of iTRAQ reagent was thawed and reconstituted in 50 μL isopropanol. Peptides

from groups were labeled with different iTRAQ tags by incubating at room temperature for 2 h. The peptide mixtures were then pooled and dried by vacuum centrifugation.

2.8. Fractionation by SCX Chromatography. For SCX chromatography, we used the HPLC (L-3120, Rigol). The peptides were eluted at a flow rate of 700 $\mu\text{L}/\text{min}$ with a gradient of buffer A (0.1% methane acid, Sigma) and then buffer B (0.1% methane acid; 80% acetonitrile, Sigma). Peptides were equilibrated with buffer A prior to the next injection. Elution was monitored by measuring absorbance at 5 min, and fractions were collected every 1.5 min. The eluted peptides were pooled as 40 fractions, freeze-centrifuged, and vacuum-dried. Labeled samples were then pooled and dried in a vacuum concentrator. The pooled mixtures of iTRAQ-labeled peptides were fractionated by strong cation-exchange chromatography (L-3120, Rigol) for LC-MS/MS.

2.9. LC-ESI-MS/MS Analysis. Each fraction was resuspended in a volume of 5 μL 0.5% FA (Sigma) and centrifuged at 14,000 g for 10 min. In each fraction, the final concentration of peptide was approximately 0.5 mg/mL on average. In total, 10 μL of each supernatant was loaded on a HPLC Ultimate 3000 (Thermo Scientific) with an autosampler onto a C18 trap column (C18 3 μm 0.10 \times 20mm), and the peptides were eluted onto an analytical C18 column (C18 1.9 μm 0.15 \times 120mm) packed in-house. The samples were loaded at 600nl/min. Data acquisition was performed with a Q-Exactive HF (Thermo Finnigan).

2.10. iTRAQ Protein Identification and Quantification. The original MS/MS file data (*.RAW) were analyzed with Mascot 2.1 and Proteome Discoverer 1.4 (Thermo) using the Rat database download from Uniprot database on Apr. 15th, 2016. The search parameters included the following: Enzyme = Trypsin; Max Missed Cleavages = 2; Fixed modifications = Carbamidomethyl (C); Variable modifications = Oxidation (M), Acetyl (Protein N-term), iTRAQ8plex (N-term), iTRAQ8plex (K), and iTRAQ8plex (Y); Peptide Mass Tolerance = \pm 15 ppm; Fragment Mass Tolerance = 20mmu; peptide confidence = high. Peptide FDR \leq 0.01 was used as the identification standard. A 1.2-fold cutoff was set to identify upregulated and downregulated proteins.

2.11. Bioinformatics Analysis. The proteins were analyzed using on-line analysis tools. Gene ontology (GO) and KEGG pathway analyses were performed through the STRING website (<http://string-db.org/>), and separate figures were produced for biological process, molecular function, and cellular component categories. The differentially expressed protein-protein network was analyzed by STRING website (<http://string-db.org/>) and the figure was also produced by the software.

2.12. Statistical Analysis. All data are expressed as the mean \pm SEM. Differences in body weight change, sucrose preference rate, time in center zone, and total travel distance between groups (control, CUMS, and EA groups) were evaluated for

statistically significant differences using One-way analysis of variance (ANOVA) followed by Least-Significant Difference (LSD) post hoc tests, or Dunnett-T post hoc test, if there was heteroscedasticity presence (SPSS software, Version20.0, SPSS Inc., USA). $P < 0.05$ was considered statistically significant.

3. Results

3.1. EA Accelerates SSRI's Antidepressant Effects in Depressed Rats. After a 21-day chronic unpredictable mild stress (CUMS) paradigm, rats underwent EA at GV20 and GV29 or EA+SSRI for 7 days (Figures 1(a)-1(b)). And we used behavioral tests to assess therapeutic effects. Body weight, sucrose preference test (SPT), and open field test (OFT) were used to assay appetite, anhedonia, and anxiety change, respectively.

After 7-day interventions, we found that EA alone has similar effects as SSRI in decreasing anhedonia and anxiety (Figures 1(c)-1(f)). In body weight changing, SSRI performed better than EA and EA+SSRI (Figure 1(c)). Additionally, EA had additive benefits when combined with SSRI compared with medication alone in decreasing anhedonia and anxiety, which consist with our previous trial results. For instance, compared with group EA or SSRI, weight, sucrose preference rate, travel distance, and central zone time spent of group EA+SSRI were significantly increased (Figures 1(d)-1(f)). Thus, these results suggest that combination of EA with SSRI improves anhedonia and anxiety in depression better than EA or SSRI alone. SSRI alone increases weight better than EA or EA+SSRI.

To further ascertain the efficacy of the EA and EA+SSRI, the histopathology of hippocampus was evaluated with HE stains. In control group, the hippocampal pyramidal cell layer in cornu Ammonis (CA) 1 is thick; cells are densely, closely, and regularly arranged; the cellular structure is complete with a clear edge. In CUMS group, the hippocampal pyramidal cell layer is thin; intercellular spaces are widened; cells are irregularly and loosely arranged; the cellular structure is incomplete, even with loss of large amounts of cells, indicating that the hippocampal tissue was damaged and cell apoptosis occurred in CUMS group. In SSRI, EA, and EA+SSRI groups, the hippocampal pyramidal cell layer is restored and intercellular spaces are narrowed to some extent, indicating rehabilitative effect against damage in the hippocampus (Figure 1(g)).

3.2. EA+SSRI Reverses Neuron Ultrastructure Pathology in Hippocampus of Depressed Rats. Increasing evidence shows that the biological mechanism of depression lies in synaptic plasticity, especially in prefrontal cortex and hippocampus [18, 19]. To investigate the role of EA in CUMS-induced synaptic plasticity change, we examined the ultrastructure of hippocampal synapse through transmission electron microscopy. Significant loss of PSD was observed in CUMS rats. Both EA and SSRI alone reversed the loss while EA caused a more significant increase in PSD. When combined with SSRI, EA caused more PSD increase compared with

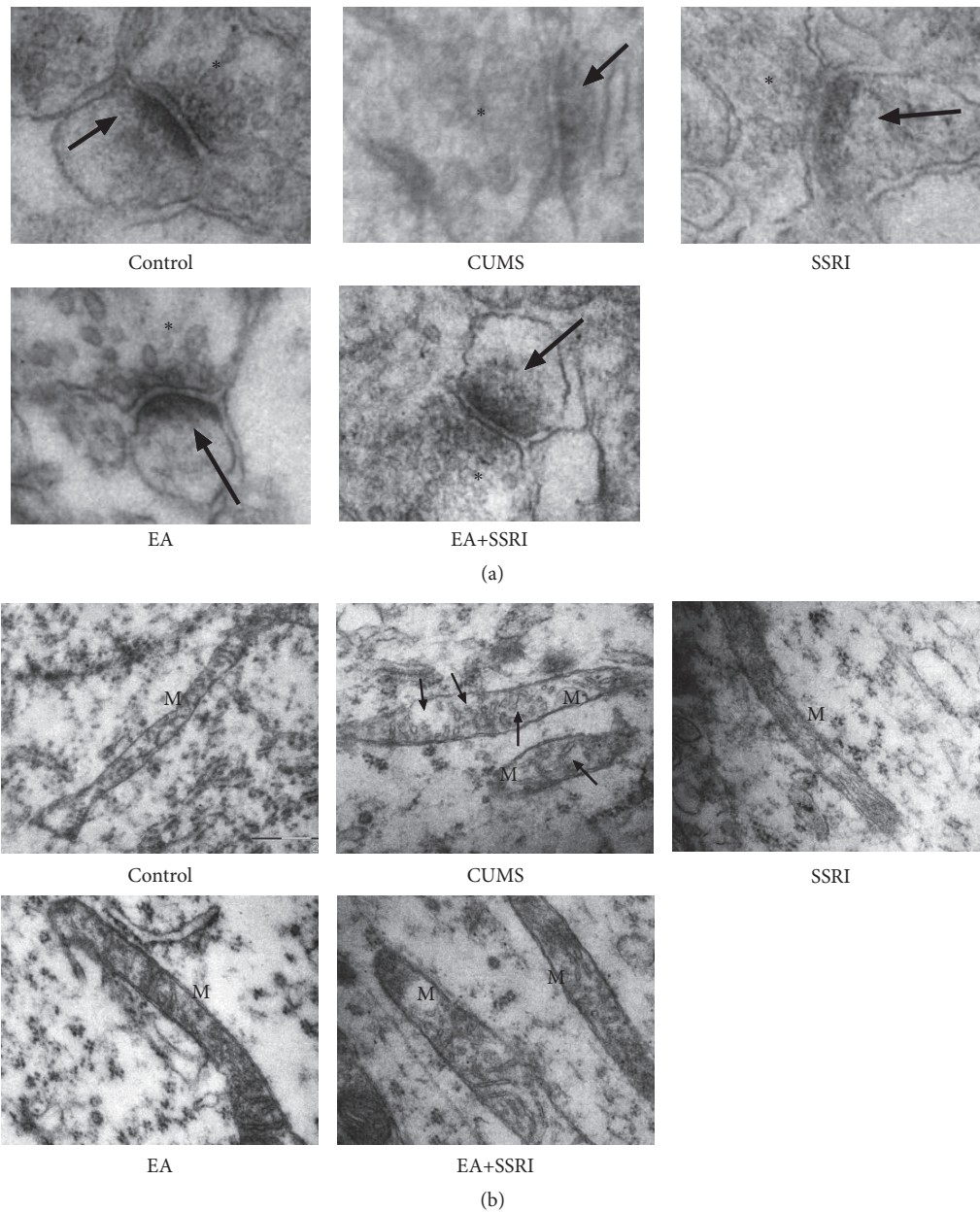


FIGURE 2: EA+SSRI reverses postsynaptic density loss and mitochondrial lesion during depression. (a) CUMS caused PSD loss in hippocampal neuron. EA and SSRI alone reversed the loss while EA was more effective. EA+SSRI induced more PSD increase compared with EA or SSRI alone. Asterisks (*): presynaptic vesicles; arrowheads: postsynaptic density (n = 3 rats/group); $\times 80,000$. (b) Exposed to CUMS, mitochondria in hippocampal neuron were enlarged and contain fragments of cristae. EA, SSRI, and EA+SSRI reversed mitochondrial damage (n = 3 rats/group). M: mitochondria. Arrowheads: cristae dissolve; $\times 24,000$.

EA or SSRI alone (Figure 2(a)). These findings suggest that synaptic plasticity especially postsynaptic structure is changed during interventions. EA, SSRI, and combination of EA with SSRI reverse PSD loss caused by CUMS, and combination treatment has the best effects.

We also found that, exposed to CUMS, mitochondrial ultrastructures in hippocampal neuron were also damaged. Normally, mitochondria are rod shaped organelles with double membrane bound (the outer membrane and the inner membrane). CUMS caused mitochondria to enlarge and

cristae dissolve and disappear leaving empty intermembrane space. EA, SSRI, and combination of them provoked mitochondria repair (Figure 2(b)). These findings indicate that mitochondria repair is also involved in the regulation of EA against depression.

3.3. EA Changes Hippocampus Proteomics Profiles of Depressive Rats. To investigate the molecular mechanisms underlying the effects of EA in depression, we examined the

TABLE 1: Differentially expressed proteins numbers between groups.

Compared groups	Upregulated protein number	Downregulated protein number
EA/CUMS	145	129

differentially expressed hippocampal proteins between control, CUMS, and EA groups through iTRAQ and used bioinformatics analysis methods to understand proteomics characters variations.

The protein abundance of 274 proteins (145 upregulated and 129 downregulated) identified with iTRAQ-based technology showed greater than a 1.2-fold change or less than a 0.83-fold change when comparing EA to CUMS rats, as well as 52 proteins (52 upregulated and 22 downregulated) when comparing CUMS to control (Table 1).

3.3.1. Categorization of Differential Proteins. To understand variations in the proteomic characteristics of differentially expressed hippocampal proteins between CUMS and EA, differentially expressed proteins were subjected to GO analysis in the STRING website (version 10). The results show that, in terms of biological process, most of the differential expressed proteins were mainly involved in cell development (8.30%, $P=0.03$), cellular component morphogenesis (6.32%, $P=0.04$), tissue development (5.53%, $P=0.01$), monovalent inorganic cation transport (5.53%, $P=0.01$), anatomical structure formation involved in morphogenesis (4.74%, $P=0.01$), proton transport (3.55%, $P=0.01$), hydrogen transport (3.55%, $P=0.01$), hydrogen ion transmembrane transport (3.55%, $P=0.01$), regulation of cell cycle process (3.16%, $P=0.01$), and regulation of mitotic cell cycle (2.371542%, $P=0.04$) (Figure 3(a)). Regarding molecular function, most of the differential proteins were annotated as being associated with transporter activity (11.46%, $P=0.04$), peptidase activity (5.92%, $P=0.03$), peptidase activity, acting on L-amino acid peptides (5.53%, $P=0.04$), monovalent inorganic cation transmembrane transporter activity (4.74%, $P=0.03$), hydrogen ion transmembrane transporter activity (3.55%, $P<0.01$), oxidoreductase activity, acting on NAD(P)H (2.76%, $P=0.02$), endopeptidase regulator activity (2.37%, $P=0.03$), NADH dehydrogenase activity (2.37%, $P=0.01$), oxidoreductase activity, acting on a heme group of donors, oxygen as acceptor (2.37%, $P<0.001$), oxidoreductase activity, and acting on a heme group of donors (2.37%, $P<0.001$) (Figure 3(b)). In terms of cellular component, most of the differential proteins are predicted to be in macromolecular complex (35.96%, $P=0.03$), membrane protein complex (11.85%, $P=0.045781$), mitochondrial membrane (9.88%, $P=0.04$), mitochondrial membrane part (4.74%, $P=0.04$), plasma membrane protein complex (4.74%, $P=0.03$), myelin sheath (4.74%, $P=0.03$), cell surface (3.95%, $P=0.02$), respiratory chain (3.55%, $P=0.01$), oxidoreductase complex (3.16%, $P=0.04$), and mitochondrial respiratory chain (3.16%, $P=0.01$) (Figure 3(c)).

3.3.2. Pathways Relevant to Differential Hippocampal Proteins. To explore the connection of differential proteins between

CUMS and EA hippocampus, KEGG pathway mapping was analyzed. KEGG pathway mapping revealed 5 significant pathways involved in EA-CUMS comparison (Table 2). The pathways were nonalcoholic fatty liver disease (NAFLD) (12 proteins, $P<0.001$), oxidative phosphorylation (12 proteins, $P<0.01$), Parkinson's disease (12 proteins, $P<0.01$), Alzheimer's disease (11 proteins, $P=0.01$), and Huntington's disease (10 proteins, $P=0.03$). Protein-protein interactions identified between groups were also noted among the differential proteins (>1.2 -fold or <0.83 -fold) (Figure 3(d)). String analyses show that the network of EA/CUMS has significantly more interactions than expected.

3.3.3. Synaptic and Mitochondria Proteins Are Involved in EA Intervention. Based on ultrastructure study findings, we focused on differential expressed protein in mitochondrion and synapse. Consisting with the transmission electron microscopy results, a total of 16 synaptic proteins were significantly changed by EA, among which 9 of them were upregulated and 7 were downregulated (with all proteins shown in Supplementary Data Tables 1 and 2). These proteins are mainly distributed in PSD and synaptic vesicle. 6 out of 16 proteins concerning PSD were changed, and 4 of them were upregulated, while 2 were downregulated; 5 synaptic vesicle proteins changed after EA, among which 2 were upregulated, while 3 were downregulated (Figure 4(a)).

On the other hand, 48 mitochondrial proteins changed after EA, of which 26 of them were upregulated and 22 were downregulated (with all proteins shown in Supplementary Data Tables 3 and 4). Interestingly, mitochondrial electron transport chain proteins alterations were rather distinct. 2 of the proteins consisting of NADH dehydrogenase were upregulated, while 5 were downregulated. In cytochrome c oxidase, 1 was upregulated, while 4 were downregulated. Only 1 protein that belongs to ATP synthase changed and it was upregulated (Figure 4(b)).

4. Discussion

Due to increasing concerns regarding the delay of antidepressant's effects, clinical researches posed a complimentary therapy combination strategy to overcome this, to combine SSRI with EA [7]. The combination therapy can bring the symptoms relief front to within 1 week [8, 9]. In this study, we showed that EA shortens the time lag of SSRI's effects. We also showed that EA has similar effects as SSRI in reducing anhedonia and anxiety as well as increasing bodyweight.

Notably, in bodyweight increasing, SSRIs precede EA and EA+SSRI. As a matter of fact, antidepressants, such as tricyclic antidepressants (TCAs) and SSRIs, are often related to weight gain in both acute and long-term treatments [38]. Paroxetine, SSRI used in this research, is associated with a greater risk of weight gain among antidepressants [39]. Thus, SSRIs may be a more favorable weight alternative than EA in patients who have significant weight loss. Still, EA+SSRI had less weight gain than SSRI. We therefore accumulate that EA may have more complicated effects on body weight in depression.

TABLE 2: KEGG analysis of differential expressed proteins between EA and CUMS rats.

ID	KEGG Pathway	Protein number	P value
ko04932	Nonalcoholic fatty liver disease (NAFLD)	12	<0.001
ko00190	Oxidative phosphorylation	12	<0.01
ko05012	Parkinson's disease	12	<0.01
ko05010	Alzheimer's disease	11	0.01
ko05016	Huntington's disease	10	0.03

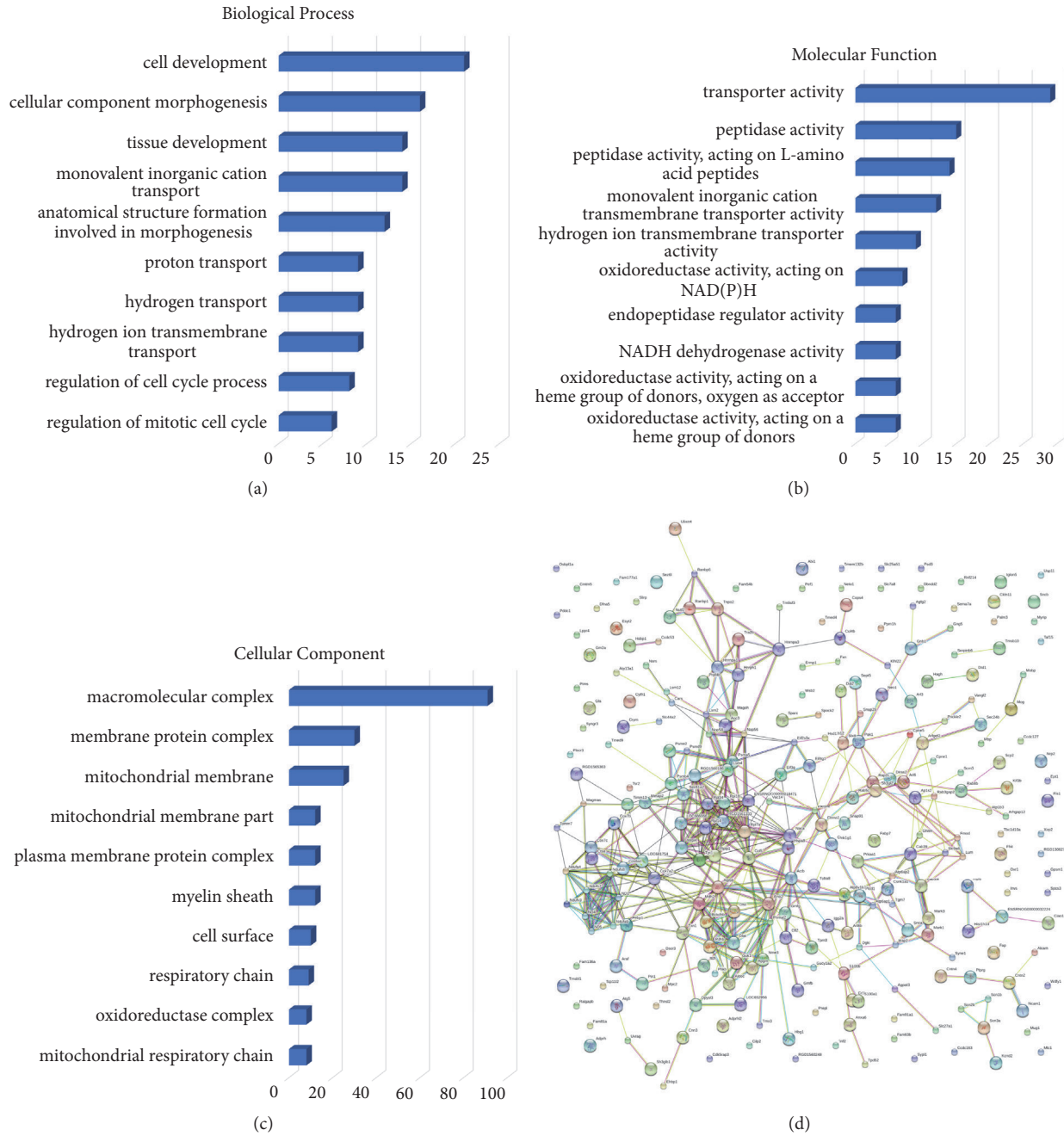


FIGURE 3: EA changes hippocampus proteomics characters in depressed rats. (a)-(c) Bar charts of the GO annotation of different proteins comparing groups. Figures (a), (b), and (c) denote biological process, cellular component, and molecular function of differential expressed proteins between CUMS and control rats' hippocampus, respectively. Scale bar: number of proteins. (b) Protein-protein interactions identified comparing EA and CUMS groups. Network of EA/CUMS has significantly more interactions than expected in STRING analysis. Network nodes: proteins; edges: associations (stronger associations are represented by thicker lines).

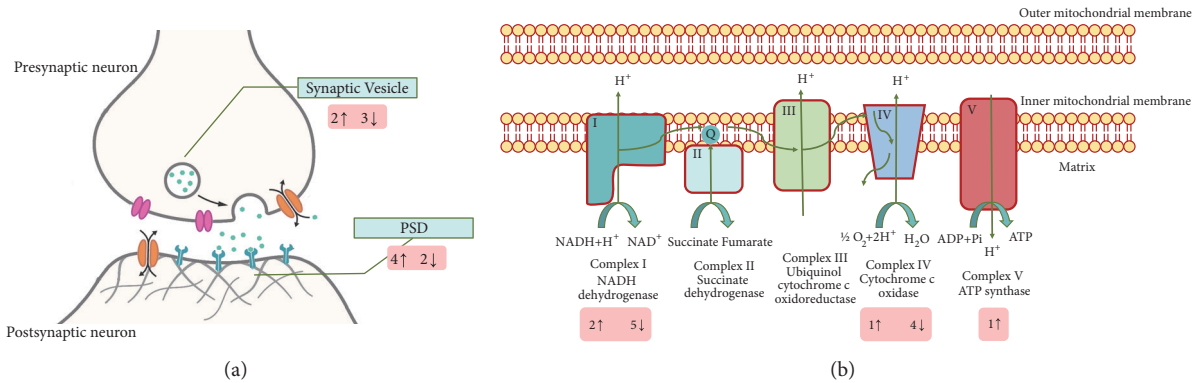


FIGURE 4: EA causes synaptic proteins and mitochondrial electron transport chain proteins change in depressed rats. (a) Synaptic proteins EA changed are mainly involved in PSD and synaptic vesicle. 5 synaptic vesicle proteins changed after EA, among which 2 were upregulated, while 3 were downregulated. 6 proteins concerning PSD were changed, and 4 of them were upregulated, while 2 were downregulated. (b) Among the differential expressed proteins distributed in mitochondria 2 of the proteins that consist of NADH dehydrogenase were upregulated while 5 were downregulated. In cytochrome c oxidase, 1 was upregulated, while 4 were downregulated. Only 1 protein that belongs to ATP synthase changed and it was upregulated. ↑: upregulated protein number. ↓: downregulated protein number. PSD: postsynaptic density.

At excitatory synapses throughout the central nervous system, the molecular composition of the postsynaptic membrane is a key determinant of synaptic strength [40]. It is a huge protein complex associated with postsynaptic membranes of excitatory synapses composed of more than 1,000 proteins including receptors, scaffold proteins, signaling enzymes, and cytoskeletal proteins. These proteins are crucial for synaptic transmission and plasticity [41]. Increasing evidence shows that the depression and acting mechanism of EA are related to altered synaptic plasticity, especially in hippocampus [18, 19, 21–23]. Synaptic changes are determined by pre- and postsynaptic structures changes such as axonal bouton, dendritic spine, and PSD [42]. In our research, we have shown that EA and EA-SSRI combination reverse PSD loss caused by CUMS in hippocampal neuron. It is accompanied by PSD proteins change, confirming that hippocampal synaptic plasticity is involved in EA's effects. Although researches before find that EA works by altering serotonin or glutamate receptor proteins, we did not observe that these proteins changed after EA. On the other hand, postsynaptic scaffold proteins are mainly involved. We speculate that the difference came from intervention time, which of these researches were all above 3 weeks. In this study we only conducted EA intervention for 1 week. Regarding the major function of scaffold proteins which is anchoring and clustering receptors proteins [43], we expect receptor proteins to change following alteration of these scaffold proteins.

Mitochondria are highly dynamic organelles that divide, fuse, and move purposefully within axons and dendrites [44]. Mitochondrial electron transport generates the ATP which is essential for the excitability and survival of neurons and the protein phosphorylation reactions that mediate synaptic signaling and related long-term changes in neuronal structure and function [45]. In this research, we also find that EA reverses mitochondrial damage in hippocampal neuron during CUMS exposure. iTRAQ data reveal that the process is accompanied by electron transport chain

changes, where NADH dehydrogenase changes significantly. This is an original study which shows that EA has protective effects on hippocampal mitochondrion. Regarding synaptic plasticity regulation which is one of the major functions of mitochondria in neurons, we assume mitochondria a possible important target of EA's synaptic plasticity mechanism.

As a matter of fact, mitochondria are essential organelles for synaptic plasticity. In synapse, mitochondria serve as energy/ATP supplier and calcium buffer organelles for long-term potentiation (LTP, effects show when synapse strengthens). On the other hand, the strengthening of synapse also promotes mitochondrial function and therefore increases ATP generation [46]. Moreover, altered mitochondrial membrane permeabilization releases cytochrome c (cyt-c). This activates caspase cascades (the intrinsic pathway), which then causes synaptic pruning (elimination of synapses) and induces long-term depression (LTD, effects shown when synapse weakens) [47]. Synaptic plasticity forms LTP and LTD are NMDA and AMPA receptors-dependent. AMPAR internalization and insertion in postsynaptic membrane and stabilization in PSD appear to be the primary cell biological mechanism underlying LTP and LTD. It is shown that AMPAR is caspase substrates. However, the exact mechanism of how caspase controls AMPAR trafficking is still unclear [48]. In our research, EA is shown to protect both mitochondria and synapse integrity in depressed hippocampus. Regarding the importance of mitochondria in synaptic plasticity, we assume that EA accelerates antidepressant effects by protecting synaptic plasticity in hippocampus via mitochondria.

Interestingly, although SSRI alone has less impact on increasing PSD than EA alone (Figure 2(a)), the effects of EA and SSRI on depressive symptoms remain similar in all behavioral tests, suggesting that the underlying mechanism of EA and SSRI may not be exactly the same. As a matter of fact, although SSRIs are generally believed to increase the level of serotonin in the synaptic cleft by limiting

its reabsorption (reuptake) into the presynaptic cell, they have varying degrees of affinity for the other monoamine transporters [49, 50]. Therefore, their exact mechanism of action remains elusive. Recent researches suggest that SSRIs improve depression through anti-inflammatory [51–53]. In this study we also show that SSRI (Paroxetine) increases PSD and protects mitochondrion in hippocampal neuron, providing new insights for mechanism of SSRIs.

Despite the different synaptic or mitochondrial proteins, 30.29% (83) different proteins locate in cytoplasm, 29.93% (82) in membrane, part of which relate to synapse. We also find that clusters of protein network relate to protein synthesis (19 proteins, of which 5 are ribosome proteins, all upregulated), cell motility (19 proteins), and translation (14 proteins). To this day, we cannot find any evidence connecting these proteins with depression. The role of these proteins in EA anti-depression effects needs to be further discussed.

Thus, this research provides a strategy to overcome the effects delay of SSRI, to combine with EA. We also proposed EA as an alternative monotherapy therapy for depression. Moreover, it provides a valuable clinical reference concerning the mechanism of EA anti-depression; that is, EA changes hippocampal synaptic and mitochondrial proteomics profiles. In depressed hippocampus, synapse and mitochondrion may be the target organelles of EA. Our findings also show that altering hippocampal synaptic plasticity may be involved in the mechanism of SSRI.

Possible limitations of the study include the fact that the exact crucial protein that responds to EA's synaptic plasticity effects needs further discussion and verification. The connection between synapse and mitochondrion in EA intervention remains inconclusive, which requires further researches in the future. We hypothesized that EA reduces CUM-induced PSD loss through protecting mitochondria functions. Still, the exact mechanism remains to be further looked into, but the functions of electron transport chain located in mitochondrial inner membrane may be a promising direction. Besides, in the experiments, we used the whole hippocampus, which includes dentate gyrus (DG), CA1, CA2, CA3, and CA4. Regarding the fact that most of the results in this research are involved in synaptic plasticity, we would like to focus on CA1 and DG next time, for synaptic plasticity in CA1 is rather vulnerable in diseases and adult neurogenesis still exists in DG, which made DG a high synaptic plasticity subfield.

Data Availability

The datasets used and analyzed during the current study are available from the corresponding author on reasonable request.

Ethical Approval

The experiment conducted in this study was approved by the Southern Medical University Experimental Animal Ethics Committee (resolution NO. L2015056).

Disclosure

Jialing Zhang is the first author and Zhinan Zhang is the co-first author.

Conflicts of Interest

The authors declare no conflicts of interest in the present study.

Authors' Contributions

Jialing Zhang, Zheng Zhong, Shanshan Qu, and Yong Huang conceived and designed the experiments. Jiping Zhang and Zengyu Yao performed the experiments. Zhinan Zhang analyzed the data.

Acknowledgments

This work was supported by the Department of Science and Technology of Guangdong Province (Grant No. 2013A032500001), Natural Science Foundation of Guangdong Province (Grant No. 2016A030313522 and 2016A030310383), National Natural Science Foundation of China (Grant No. 81603474 and 81873359), Science and Technology Program of Guangzhou (Grant No. 201707010041) and Dean's Funding Project of 2018, Nanfang Hospital, Southern Medical University (Grant No. 2018Z023), China. The authors wish to acknowledge the cooperation of the Department of Laboratory Animal Center of Southern Medical University. Meanwhile, gratitude should also be given to all those who generously contributed their time and efforts into this experiment and the paper.

Supplementary Materials

Table 1: Upregulated synaptic proteins compared EA to CUMS. Table 2: Downregulated synaptic proteins compared EA to CUMS. Table 3: Upregulated mitochondrial proteins compared EA to CUMS. Table 4: Downregulated mitochondrial proteins compared EA to CUMS. Graphic abstract: EA: EA. Hipp: hippocampus. PSD: postsynaptic density. (*Supplementary Materials*)

References

- [1] H. R. Amick, G. Gartlehner, B. N. Gaynes et al., "Comparative benefits and harms of second generation antidepressants and cognitive behavioral therapies in initial treatment of major depressive disorder: Systematic review and meta-analysis," *BMJ*, vol. 351, article h6019, 2015.
- [2] A. Khan, J. Faucett, P. Lichtenberg, I. Kirsch, and W. A. Brown, "A systematic review of comparative efficacy of treatments and controls for depression," *PLoS ONE*, vol. 7, no. 7, article e41778, 2012.
- [3] J. C. Jakobsen, K. K. Katakam, A. Schou et al., "Selective serotonin reuptake inhibitors versus placebo in patients with major depressive disorder. a systematic review with

- meta-analysis and trial sequential analysis," *BMC Psychiatry*, vol. 17, no. 1, article no. 58, 2017.
- [4] B. M. Berman, H. H. Langevin, C. M. Witt, and R. Dubner, "Acupuncture for chronic low back pain," *The New England Journal of Medicine*, vol. 363, no. 5, pp. 454–461, 2010.
 - [5] M. Kokosar, A. Benrick, A. Perilyev et al., "A single bout of electroacupuncture remodels epigenetic and transcriptional changes in adipose tissue in polycystic ovary syndrome," *Scientific Reports*, vol. 8, no. 1, article 1878, 2018.
 - [6] Jian Yang, Yu Pei, Yan-L Pan I et al., "Enhanced antidepressant-like effects of electroacupuncture combined with citalopram in a rat model of depression," *Evidence-Based Complementary and Alternative Medicine*, vol. 2013, Article ID 107380, 12 pages, 2013.
 - [7] D.-M. Duan, Y. Tu, L.-P. Chen, and Z.-J. Wu, "Efficacy evaluation for depression with somatic symptoms treated by electroacupuncture combined with fluoxetine," *Journal of Traditional Chinese Medicine*, vol. 29, no. 3, pp. 167–173, 2009.
 - [8] S. H. Ma, S. S. Qu, Y. Huang et al., "Improvement in quality of life in depressed patients following verum acupuncture or electroacupuncture plus paroxetine: a randomized controlled study of 157 cases," *Neural Regeneration Research*, vol. 7, no. 27, pp. 2123–2129, 2012.
 - [9] S.-S. Qu, Y. Huang, Z.-J. Zhang et al., "A 6-week randomized controlled trial with 4-week follow-up of acupuncture combined with paroxetine in patients with major depressive disorder," *Journal of Psychiatric Research*, vol. 47, no. 6, pp. 726–732, 2013.
 - [10] J. Cole, S. G. Costafreda, P. McGuffin, and C. H. Y. Fu, "Hippocampal atrophy in first episode depression: a meta-analysis of magnetic resonance imaging studies," *Journal of Affective Disorders*, vol. 134, no. 1–3, pp. 483–487, 2011.
 - [11] P. Videbeck and B. Ravnkilde, "Hippocampal volume and depression: a meta-analysis of MRI studies," *The American Journal of Psychiatry*, vol. 161, no. 11, pp. 1957–1966, 2004.
 - [12] P. Willner, J. Scheel-Krüger, and C. Belzung, "The neurobiology of depression and antidepressant action," *Neuroscience & Biobehavioral Reviews*, vol. 37, no. 10, pp. 2331–2371, 2013.
 - [13] G. Zhang, S. Qu, and Y. Zheng, "Key regions of the cerebral network are altered after electro acupuncture at the Baihui (GV20) and Yintang acupuncture points in healthy volunteers: an analysis based on resting fMRI," *Acupuncture in Medicine*, vol. 31, no. 4, pp. 383–388, 2013.
 - [14] D.-M. Duan, Y. Tu, S. Jiao, and W. Qin, "The relevance between symptoms and magnetic resonance imaging analysis of the hippocampus of depressed patients given electro-acupuncture combined with fluoxetine intervention—a randomized, controlled trial," *Chinese Journal of Integrative Medicine*, vol. 17, no. 3, pp. 190–199, 2011.
 - [15] D.-M. Duan, Y. Tu, L.-P. Chen, and Z.-J. Wu, "Study on electroacupuncture treatment of depression by magnetic resonance imaging," *Zhongguo Zhen Jiu = Chinese Acupuncture & Moxibustion*, vol. 29, no. 2, pp. 139–144, 2009.
 - [16] G. Neves, S. F. Cooke, and T. V. P. Bliss, "Synaptic plasticity, memory and the hippocampus: a neural network approach to causality," *Nature Reviews Neuroscience*, vol. 9, no. 1, pp. 65–75, 2008.
 - [17] D. M. Bannerman, R. Sprengel, D. J. Sanderson et al., "Hippocampal synaptic plasticity, spatial memory and anxiety," *Nature Reviews Neuroscience*, vol. 15, no. 3, pp. 181–192, 2014.
 - [18] C. Pittenger and R. S. Duman, "Stress, depression, and neuroplasticity: a convergence of mechanisms," *Neuropsychopharmacology*, vol. 33, no. 1, pp. 88–109, 2008.
 - [19] R. S. Duman, G. K. Aghajanian, G. Sanacora, and J. H. Krystal, "Synaptic plasticity and depression: new insights from stress and rapid-acting antidepressants," *Nature Medicine*, vol. 22, no. 3, pp. 238–249, 2016.
 - [20] A. Lee, Y. Hirabayashi, S.-K. Kwon, T. L. Lewis, and F. Polleux, "Emerging roles of mitochondria in synaptic transmission and neurodegeneration," *Current Opinion in Physiology*, vol. 3, pp. 82–93, 2018.
 - [21] X. Han, H. Wu, P. Yin et al., "Electroacupuncture restores hippocampal synaptic plasticity via modulation of 5-HT receptors in a rat model of depression," *Brain Research Bulletin*, vol. 139, pp. 256–262, 2018.
 - [22] Y. She, J. Xu, Y. Duan et al., "Possible antidepressant effects and mechanism of electroacupuncture in behaviors and hippocampal synaptic plasticity in a depression rat model," *Brain Research*, vol. 1629, pp. 291–297, 2015.
 - [23] D. Luo, R. Ma, Y. Wu et al., "Mechanism underlying acupuncture-ameliorated depressive behaviors by enhancing glial glutamate transporter in chronic unpredictable mild stress (CUMS) rats," *Medical Science Monitor*, vol. 23, pp. 3080–3087, 2017.
 - [24] W.-Y. Bao, S. Jiao, J. Lu et al., "Effect of electroacupuncture intervention on learning-memory ability and injured hippocampal neurons in depression rats," *Zhongguo Yi Xue Ke Xue Yuan Yi Xue Qing Bao Yan Jiu Suo Bian Ji*, vol. 39, no. 2, pp. 136–141, 2014.
 - [25] M. Bantscheff, M. Schirle, G. Sweetman, J. Rick, and B. Kuster, "Quantitative mass spectrometry in proteomics: a critical review," *Analytical and Bioanalytical Chemistry*, vol. 389, no. 4, pp. 1017–1031, 2007.
 - [26] A.-C. Gingras, M. Gstaiger, B. Raught, and R. Aebersold, "Analysis of protein complexes using mass spectrometry," *Nature Reviews Molecular Cell Biology*, vol. 8, no. 8, pp. 645–654, 2007.
 - [27] T. Wytenbach and M. T. Bowers, "Intermolecular interactions in biomolecular systems examined by mass spectrometry," *Annual Review of Physical Chemistry*, vol. 58, pp. 511–533, 2007.
 - [28] S. G. Chee, K. C. Poh, K. P. Trong, and P. C. Wright, "Technical, experimental, and biological variations in isobaric tags for relative and absolute quantitation (iTRAQ)," *Journal of Proteome Research*, vol. 6, no. 2, pp. 821–827, 2007.
 - [29] S. Yi, S. Lin, Y. Li, W. Zhao, G. B. Mills, and N. Sahni, "Functional variomics and network perturbation: Connecting genotype to phenotype in cancer," *Nature Reviews Genetics*, vol. 18, no. 7, pp. 395–410, 2017.
 - [30] M. Frantzi, A. Latosinska, L. Flühe et al., "Developing proteomic biomarkers for bladder cancer: towards clinical application," *Nature Reviews Urology*, vol. 12, no. 6, pp. 317–330, 2015.
 - [31] M. Zhou, M. Wang, X. Wang et al., "Abnormal expression of micRNAs induced by chronic unpredictable mild stress in rat hippocampal tissues," *Molecular Neurobiology*, vol. 55, no. 2, pp. 917–935, 2018.
 - [32] N. Wang, H.-Y. Yu, X.-F. Shen et al., "The rapid antidepressant effect of ketamine in rats is associated with down-regulation of pro-inflammatory cytokines in the hippocampus," *Upsala Journal of Medical Sciences*, vol. 120, no. 4, pp. 241–248, 2015.
 - [33] W. Li, Y. Zhu, S. M. Saud et al., "Electroacupuncture relieves depression-like symptoms in rats exposed to chronic unpredictable mild stress by activating ERK signaling pathway," *Neuroscience Letters*, vol. 642, pp. 43–50, 2017.
 - [34] H.-M. Qiu, J.-X. Yang, X.-H. Wu et al., "Antidepressive effect of paroxetine in a rat model: upregulating expression of serotonin

- and norepinephrine transporter,” *NeuroReport*, vol. 24, no. 10, pp. 520–525, 2013.
- [35] K. J. Tuerke, F. Leri, and L. A. Parker, “Antidepressant-like effects of paroxetine are produced by lower doses than those which produce nausea,” *Pharmacology Biochemistry & Behavior*, vol. 93, no. 2, pp. 190–195, 2009.
- [36] J. Lu, R.-H. Shao, S.-Y. Jin, L. Hu, Y. Tu, and J.-Y. Guo, “Acupuncture ameliorates inflammatory response in a chronic unpredictable stress rat model of depression,” *Brain Research Bulletin*, vol. 128, pp. 106–112, 2017.
- [37] X. Zhu, G. Ye, Z. Wang, J. Luo, and X. Hao, “Sub-anesthetic doses of ketamine exert antidepressant-like effects and upregulate the expression of glutamate transporters in the hippocampus of rats,” *Neuroscience Letters*, vol. 639, pp. 132–137, 2017.
- [38] M. Fava, “Weight gain and antidepressants,” *Journal of Clinical Psychiatry*, vol. 61, no. 11, pp. 37–41, 2000.
- [39] A. Serretti and L. Mandelli, “Antidepressants and body weight: a comprehensive review and meta-analysis,” *Journal of Clinical Psychiatry*, vol. 71, no. 10, pp. 1259–1272, 2010.
- [40] B. L. Sinnen, A. B. Bowen, J. S. Forte et al., “Optogenetic Control of Synaptic Composition and Function,” *Neuron*, vol. 93, no. 3, pp. 646–660, 2017.
- [41] T. Kaizuka and T. Takumi, “Postsynaptic density proteins and their involvement in neurodevelopmental disorders,” *The Journal of Biochemistry*, vol. 163, no. 6, pp. 447–455, 2018.
- [42] D. Meyer, T. Bonhoeffer, and V. Scheuss, “Balance and stability of synaptic structures during synaptic plasticity,” *Neuron*, vol. 82, no. 2, pp. 430–443, 2014.
- [43] C. Verpelli, M. J. Schmeisser, C. Sala, and T. M. Boeckers, “Scaffold proteins at the postsynaptic density,” *Advances in Experimental Medicine and Biology*, vol. 970, pp. 29–61, 2012.
- [44] E. L. Streck, C. L. Gonçalves, C. B. Furlanetto, G. Scaini, F. Dal-Pizzol, and J. Quevedo, “Mitochondria and the central nervous system: searching for a pathophysiological basis of psychiatric disorders,” *Revista Brasileira de Psiquiatria*, vol. 36, no. 2, pp. 156–167, 2014.
- [45] M. P. Mattson, M. Gleichmann, and A. Cheng, “Mitochondria in neuroplasticity and neurological disorders,” *Neuron*, vol. 60, no. 5, pp. 748–766, 2008.
- [46] V. Todorova and A. Blokland, “Mitochondria and synaptic plasticity in the mature and aging nervous system,” *Current Neuropharmacology*, vol. 15, no. 1, pp. 166–173, 2017.
- [47] A. Mukherjee and D. W. Williams, “More alive than dead: non-apoptotic roles for caspases in neuronal development, plasticity and disease,” *Cell Death & Differentiation*, vol. 24, no. 8, pp. 1411–1421, 2017.
- [48] Z. Li and M. Sheng, “Caspases in synaptic plasticity,” *Molecular Brain*, vol. 5, no. 1, article 15, 2012.
- [49] I. Hindmarch and K. Hashimoto, “Cognition and depression: the effects of fluvoxamine, a sigma-1 receptor agonist, reconsidered,” *Journal of Psychopharmacology*, vol. 25, no. 3, pp. 193–200, 2010.
- [50] Y. Albayrak and K. Hashimoto, “Sigma-1 receptor agonists and their clinical implications in neuropsychiatric disorders,” *Advances in Experimental Medicine and Biology*, vol. 964, pp. 153–161, 2017.
- [51] P. Gałeczki, J. Mossakowska-Wójcik, and M. Talarowska, “The anti-inflammatory mechanism of antidepressants – SSRIs, SNRIs,” *Progress in Neuro-Psychopharmacology & Biological Psychiatry*, vol. 80, pp. 291–294, 2018.
- [52] S. Köhler, K. Cierpinsky, G. Kronenberg, and M. Adli, “The serotonergic system in the neurobiology of depression: Relevance for novel antidepressants,” *Journal of Psychopharmacology*, vol. 30, no. 1, pp. 13–22, 2016.
- [53] O. Köhler, J. Krogh, O. Mors, and M. E. Benros, “Inflammation in depression and the potential for anti-inflammatory treatment,” *Current Neuropharmacology*, vol. 14, no. 7, pp. 732–742, 2016.